Angular Distribution of the Photoelectron Yield Excited by Two Coherently Coupled Photon Beams

Lonny E. Berman[1] and Michael J. Bedzyk[2]

[1]*National Synchrotron Light Source, Brookhaven National Laboratory, Upton, New York 11973*

[2]*School of Applied and Engineering Physics and the Cornell High Energy Synchrotron Source, Cornell University, Ithaca, New York 14853*

(Received 5 May 1989)

The angular distribution of the photoelectron yield excited by two coherently related photon beams has been calculated and measured. Dynamical Bragg diffraction from a Ge(111) single crystal was used to generate the two beams, and L-shell photoelectron yields from an I overlayer were measured with a variable-angular-acceptance detector. The use of two-beam photoelectric excitation to understand final-state angular momentum symmetry is demonstrated.

PACS numbers: 79.60.−i, 32.80.Wr, 61.10.Jv, 78.70.Dm

The angular distribution of electrons ejected from an atom as a result of the photoelectric effect is a classic problem in quantum mechanics, one which is well understood for the case of a single primary photon beam. For instance, if the ejected electron initially has s angular momentum symmetry, and only dipole transitions are considered, then the final electron state consists of an expansion in terms of continuum wave functions to which only p partial waves contribute.[1] The resulting angular distribution has a $\cos^2\theta$ dependence relative to a polar axis which is aligned with the electric field polarization vector of the incident photon beam.[1]

In this Letter, we examine the differential photoelectric effect cross section for an atom in an external electric field arising from the superposition of two coherently related photon plane waves. Experimentally, we use dynamical Bragg x-ray diffraction from a perfect germanium crystal to prepare the two beams, and simultaneously monitor the angular distribution of L-shell photoelectrons from an ordered iodine overlayer. We also show how two-beam photoelectric excitation can be used to learn about the final-state angular momentum symmetry.

An expression for the differential cross section for the absorption of a photon plane wave by an atom, and concomitant ejection of a bound electron into a continuum final state, can be found in Bethe and Jackiw's textbook:[1]

$$\frac{d\sigma(\theta,\phi)}{d\Omega} = \frac{e^2}{2\pi mc}\frac{k_f}{\omega}\,|\langle f|\exp(2\pi i\mathbf{k}\cdot\mathbf{r})\hat{\epsilon}\cdot\nabla|n\rangle|^2 . \quad (1)$$

The photoelectron emerges in a direction specified by spherical angles θ and ϕ relative to the incident beam electric field polarization vector $\hat{\epsilon}$. The incident photon has wave vector $\mathbf{k}$ and angular frequency ω, and the photoelectron is described by wave vector k_f, initial (bound) state $|n\rangle$, and final (continuum) state $|f\rangle$. Now consider the case of two photon beams, the second one arising from diffraction from the $\mathbf{H}$ set of Bragg planes of a perfect crystal. We first recast the matrix element in Eq. (1) using the total electric field:

$$\frac{d\sigma}{d\Omega} \propto |\,\varepsilon_0\langle f|\exp(2\pi i\mathbf{K}_0\cdot\mathbf{r})\hat{\epsilon}_0\cdot\nabla|n\rangle + \varepsilon_H\langle f|\exp(2\pi i\mathbf{K}_H\cdot\mathbf{r})\hat{\epsilon}_H\cdot\nabla|n\rangle|^2 , \quad (2)$$

where the total field is the sum of two fields of the form

$$\varepsilon_j\hat{\epsilon}_j = E_j\exp(-i[2\pi\mathbf{K}_j\cdot\mathbf{r}-\omega t])\hat{\epsilon}_j , \quad (3)$$

with the index j being 0 for the incident beam and H for the diffracted beam. E_j is the complex electric field amplitude, $\hat{\epsilon}_j$ is the unit polarization vector, and $\mathbf{K}_j$ is the photon wave vector. Equation (2) can be simplified by using the dipole approximation to the photoelectric absorption cross section[2] ($\exp[2\pi i\mathbf{K}_j\cdot\mathbf{r}]\rightarrow 1$), Bragg's law ($\mathbf{K}_H=\mathbf{K}_0+\mathbf{H}$), and the phase v and magnitude $|E_h/E_0|$ of E_h relative to E_0 ($E_H/E_0=|E_H/E_0|\exp[iv]$), which are functionally related to the angle of incidence on the Bragg planes,[3] to obtain

$$\frac{d\sigma}{d\Omega} \propto |\langle f|\hat{\epsilon}_0\cdot\nabla|n\rangle|^2 + \left|\frac{E_H}{E_0}\right|^2|\langle f|\hat{\epsilon}_H\cdot\nabla|n\rangle|^2 + \left|\frac{E_H}{E_0}\right|\exp(i[v-2\pi\mathbf{H}\cdot\mathbf{r}])\langle f|\hat{\epsilon}_0\cdot\nabla|n\rangle^*\langle f|\hat{\epsilon}_H\cdot\nabla|n\rangle$$
$$+\left|\frac{E_H}{E_0}\right|\exp(-i[v-2\pi\mathbf{H}\cdot\mathbf{r}])\langle f|\hat{\epsilon}_0\cdot\nabla|n\rangle\langle f|\hat{\epsilon}_H\cdot\nabla|n\rangle^* . \quad (4)$$

Since we are confining our attention to photoelectrons from surface atoms, depth attenuation of the electric field, the "extinction" effect,[3] has been ignored in this treatment.

The differential cross section, $d\sigma/d\Omega$, contains separate contributions from the incident and diffracted beams acting alone, plus one of a mixed nature (last two terms). The latter arises from interference between the two outgoing photoelectron waves that are azimuthally symmetric about the incident and diffracted beam polarization vectors. In the σ polarization scattering geometry, in which the incident and diffracted electric field vectors are perpendicular to the scattering plane, $\hat{\boldsymbol{\epsilon}}_0$ and $\hat{\boldsymbol{\epsilon}}_H$ are collinear, and the matrix elements cancel out of Eq. (4);

$$\frac{d\sigma}{d\Omega} \propto 1+\left|\frac{E_H}{E_0}\right|^2+2\left|\frac{E_H}{E_0}\right|\cos(v-2\pi\mathbf{H}\cdot\mathbf{r}). \quad (5)$$

In this case, $d\sigma/d\Omega$ behaves identically with the electric field intensity at the observation point $\mathbf{r}$ as the Bragg reflection is scanned; the electric field has the form of a standing wave with nodal and antinodal planes parallel to the diffraction planes, and whose period is the interplanar spacing.[3] The standing-wave nodes shift inward from alignment with the diffraction planes to between the planes as the incidence angle is advanced through the Bragg reflection, resulting in a predictable modulation in the photoelectron yield from an atom at position $\mathbf{r}$.[4]

In the π polarization geometry, in which the incident and diffracted electric field vectors lie in the scattering plane, $\hat{\boldsymbol{\epsilon}}_0$ and $\hat{\boldsymbol{\epsilon}}_H$ are misaligned by the scattering angle $2\Theta_B$, where Θ_B is the nominal Bragg angle. Unlike the σ geometry situation, the angular momenta of the initial $|n\rangle$ and final $|f\rangle$ state electron wave functions influence the behavior of $d\sigma/d\Omega$ as the Bragg reflection is scanned; its functional dependence on the incidence angle differs from that of the electric field intensity.[5] For example, if the initial state has s angular momentum symmetry, then the final state has p symmetry (for a dipole transition) and the matrix elements in Eq. (4) have a $\cos\theta$ angular dependence with respect to the appropriate polarization vector. In this case,

$$\frac{d\sigma}{d\Omega} \propto 1+C_1\left|\frac{E_H}{E_0}\right|^2+2C_2\left|\frac{E_H}{E_0}\right|\cos(v-2\pi\mathbf{H}\cdot\mathbf{r}), \quad (6)$$

where $C_1=(\cos\theta_H/\cos\theta_0)^2$, $C_2=\cos\theta_H/\cos\theta_0$, and θ_0 and θ_H are the polar angles relative to $\hat{\boldsymbol{\epsilon}}_0$ and $\hat{\boldsymbol{\epsilon}}_H$, respectively.

Figure 1 shows the two photoelectron angular yield distributions, due to the incident and diffracted beams acting alone, in the π scattering geometry. Suppose we have an electron detector which can view the sample along the azimuths labeled 0° and 180° in Fig. 1. If we observe the photoelectron yield along the 0° azimuth as the Bragg reflection from the sample is scanned, we would expect to observe a relatively weak modulation, since this azimuth is nearly perpendicular to the diffracted beam polarization vector and thus insensitive to the yield due to the diffracted beam. Along the 180° azimuth, however, we would expect a relative strong modulation, since this azimuth is more aligned with the polarization of the diffracted beam compared with that of the incident beam.

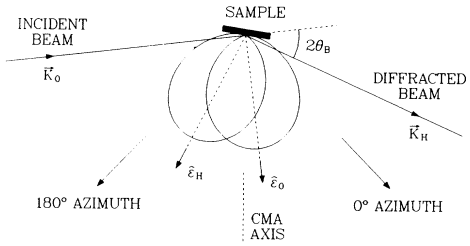

FIG. 1. The π polarization scattering geometry is shown. The polarization vectors $\hat{\boldsymbol{\epsilon}}_0$ and $\hat{\boldsymbol{\epsilon}}_H$ serve as the polar axes for the $\cos^2\theta$ photoelectron distributions (for $s\rightarrow p$ dipole transitions) due to the incident and diffracted beams acting alone, respectively. Experimentally, the CMA axis was misaligned from $\hat{\boldsymbol{\epsilon}}_0$ by 7°.

To realize these notions experimentally, we measured L-shell photoelectron yields from an I overlayer (of coverage 1.5 monolayers) deposited on a clear Ge(111) surface in ultrahigh vacuum (UHV), as the (111) reflection from the substrate was scanned in the π geometry, using a double-pass cylindrical mirror analyzer (CMA).[6] The CMA detects only those electrons emerging into a conical shell of half-angle 42.3° ± 6° relative to its axis. It has an internal rotatable annular aperture, which narrows its field of view to any 12° azimuthal-angle interval about the cone axis. Figure 1 shows the alignment of the CMA axis, as well as its 0° and 180° azimuths, relative to the x-ray scattering geometry. Further details regarding the experimental setup and surface preparation can be found in Ref. 7. The experiment was performed at the Cornell High Energy Synchrotron Source (CHESS). The white x-ray beam was monochromated by a pair of Si(111) crystals. In the range of photon energies used (6–7 keV), the CHESS x-ray beam was approximately 85% polarized in the scattering plane.

A first series of measurements was performed by monitoring the I L_I photoelectron yield, for which the initial electron state has s angular momentum symmetry. Figure 2 shows the yields measured with the CMA's annular aperture centered on the (curve a) 0° and (curve b) 180° azimuths, as well as (curve c) the yield measured with the aperture removed (i.e., integrated over the full CMA cone) as the (111) reflection was scanned. The nominal photoelectron kinetic energy was 1560 eV, and the energy resolution of the CMA was 25 eV. The lowest curve in Fig. 2 is the Ge(111) reflectivity. The theoretical yields shown as solid lines in Fig. 2 were calculated using Eq. (6). For case (a), $C_1=0.22$ and $C_2=0.47$; for case (b), $C_1=2.16$ and $C_2=1.47$; for case (c), $C_1=0.90$ and $C_2=0.88$. The theoretical yields shown as dashed lines have the same functional dependence on incidence angle as the electric field intensity,

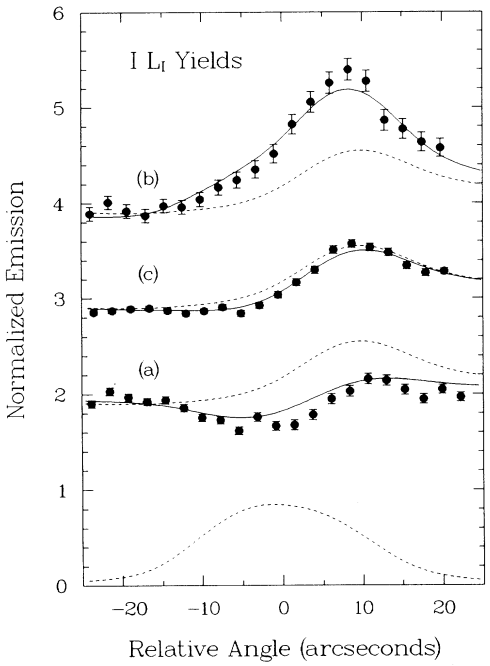

FIG. 2. Shown are the I L_I photoelectron yields, as functions of the angular misalignment between monochromator and sample relative to that at the center of the Bragg reflection, measured with the CMA annular aperture oriented to view the (curve *a*) 0° and (curve *b*) 180° azimuths, and (curve *c*) with the aperture removed. The lowest curve is the Ge(111) reflectivity. The theoretical yields shown as solid curves assume an $s \rightarrow p$ dipole transition; the ones shown as dashed curves follow the electric field intensity. Each set of curves (*a*), (*c*), and (*b*) is successively displaced by one unit along the ordinate.

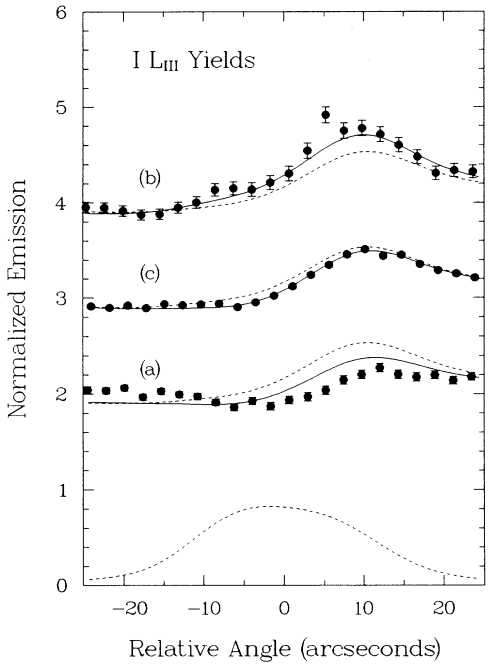

FIG. 3. Same as Fig. 2, but for the I L_{III} yields. The solid curves are the theoretical yields assuming a pure $p \rightarrow d$ dipole transition, and the dashed curves would result from a pure $p \rightarrow s$ transition; the latter follow the variation of the electric field intensity. The lowest curve is the Ge(111) reflectivity.

and were obtained by setting $C_1 = 1$ and $C_2 = \cos 2\Theta_B = 0.84$, the x-ray polarization factor,[3] in Eq. (6), for all cases.

To complete the comparison of theory and experiment, it is necessary to know the "observation" position $\mathbf{H} \cdot \mathbf{r}$ in Eq. (6). This represents the location of the I atoms with respect to the (111) diffraction planes, expressed in units of the (111) interplanar spacing. We determine this to be -0.14 ± 0.01 in a separate x-ray standing-wave measurement of the same sample in which the I *MNN* Auger yield at 490 eV was monitored;[8] this yield in fact showed no noticeable azimuthal anisotropy.[9] If the I overlayer is not perfectly ordered normal to the (111) planes, the last term in Eq. (6) must also be weighted by the fraction of I atoms which sit at the preferred position, with the remainder randomly distributed normal to the (111) planes. This fraction was determined to be 0.59 ± 0.02 from the Auger yield measurement.

The agreement between theory and experiment in Fig. 2 improves when the electron angular momenta are taken into account. The photoelectron yields show the behavior described earlier, a relatively weak modulation for the 0° azimuth and a strong one for the 180° azimuth as the Bragg reflection is scanned. The integrated yield shown in Fig. 2(c) is close to the average modulation, which follows the variation of the electric field intensity, due to the extent of solid angle averaging.[5]

We also measured I L_{III} photoelectron yields, and show the results in Fig. 3. Here, the initial electron state has *p* angular momentum symmetry. Dipole selection rules allow transitions to continuum states with pure *s* and pure *d* character, as well as states of mixed *s*-*d* character, which can arise from interference of the outgoing *s* and *d* photoelectron waves.[10] The solid lines in Fig. 3 are the yields calculated using Eq. (6), assuming a pure $p \rightarrow d$ transition. For curves (*a*), the yield observed along the 0° azimuth, $C_1 = 0.64$ and $C_2 = 0.63$; for (*b*), the yield observed along the 180° azimuth, $C_1 = 1.40$ and $C_2 = 1.03$; for (*c*), the integrated yield, $C_1 = 0.91$ and $C_2 = 0.84$. The dashed lines assume a pure $p \rightarrow s$ transition, for which $C_1 = 1$ and $C_2 = 0.81$ for all cases. We assumed no preferred alignment of the initial *p* state, which should be valid for inner electron shells. For a spherically symmetric *s* final state, of course, no azimuthal anisotropy is expected; the yield has the same dependence on incidence angle as the electric field intensity. The contrast between the yields observed at the different azimuths are not as strong as for the L_I yields, since both *s* and *d* states have less pronounced angular

features than p states. A stronger modulation is clearly seen for the 180° azimuth data compared with the 0° data, indicating that the final state is not pure s. From the comparison of the data to the theoretical curves shown in Fig. 3, it is evident that the photoelectron final state has a stronger d than s character, which is consistent with theoretical calculations[10] for the photoelectron kinetic energy used (1540 eV).

Notice that insight into the final-state symmetry can be obtained from a measurement using just one of the azimuths. In conventional angle-resolved photoemission studies of orbital symmetry,[11] using a single primary photon beam, measurements at several azimuths are usually required. Two-beam photoelectric excitation can hence be a useful tool for the study of orbital symmetry for atoms and molecules adsorbed on perfect single-crystal and multilayer surfaces.

Discussions with Jene Golovchenko, Boris Batterman, Jack Blakely, and Jerry Hastings and assistance provided by Gary Navrotski, Qun Shen, Mary Keeffe, and the CHESS staff are gratefully acknowledged. This work was supported by the NSF via Grant Nos. DMR-85-16616 and DMR-87-19764, and by the DOE via Contract No. DE-AC02-76CH00016.

[1]H. A. Bethe and R. W. Jackiw, *Intermediate Quantum Mechanics* (Benjamin Cummings, Reading, Ma, 1986), 3rd ed., Chap. 12.

[2]The dipole approximation is valid when the spatial extent of the initial (bound) electron wave function is much smaller than the x-ray wavelength, a condition which is satisfied in the reported measurements; see also Ref. 1 and H. Wagenfeld, Phys. Rev. **144**, 216 (1966).

[3]B. W. Batterman and H. Cole, Rev. Mod. Phys. **36**, 681 (1964).

[4]The application of x-ray standing waves to determine atomic positions is described in M. J. Bedzyk, D. H. Bilderback, G. M. Bommarito, M. Caffrey, and J. S. Schildkraut, Science **241**, 1788 (1988), and references therein.

[5]The total cross section, however, obtained by integrating the differential cross section over all solid angles, *does* have the same functional dependence on incidence angle as the electric field intensity.

[6]Previous experiments in which photoelectron yields were measured during Bragg diffraction were not truly surface sensitive, and thus the described yield modulations were washed out by multiple scattering of the emerging photoelectrons; see S. Kikuta, T. Takahashi, and Y. Tuzi, Phys. Lett. **50A**, 453 (1975); V. N. Shchemelev and M. V. Kruglov, Kristallografiya **20**, 251 (1975) [Sov. Phys. Crystallogr. **20**, 153 (1975)].

[7]M. J. Bedzyk, Q. Shen, M. Keeffe, G. Navrotski, and L. E. Berman, Surf. Sci. (to be published).

[8]This agrees with the result of another measurement, described in Ref. 7, in which a Ge(111) sample prepared with an I overlayer in UHV was subsequently removed from the vacuum chamber and characterized with x-ray standing waves, using the I L x-ray fluorescence yield.

[9]The Auger-electron yield is generally isotropic, with a few exceptions; see T. A. Carlson, D. R. Mullins, C. E. Beall, B. W. Yates, J. W. Taylor, D. W. Lindle, B. P. Pullen, and F. A. Grimm, Phys. Rev. Lett. **60**, 1382 (1988).

[10]S. T. Manson, J. Electron Spectrosc. **1**, 413 (1972/1973).

[11]For recent reviews of angle-resolved photoemission, see J. H. D. Eland, *Photoelectron Spectroscopy* (Butterworths, London, 1984), Chap. 3; N. V. Smith and F. J. Himpsel, in *Handbook on Synchrotron Radiation,* edited by E. E. Koch (North-Holland, Amsterdam, 1983), Vol. 1; E. W. Plummer and W. Eberhardt, Adv. Chem. Phys. **49**, 533 (1982).